Theor Chem Acc (1998) 99:241–247
DOI 10.1007/s0021498000m9

Theoretical
Chemistry Accounts

Regular article

Global geometry optimization of small silicon clusters at the level of density functional theory

Bernd Hartke

Institut für Theoretische Chemie, Universität Stuttgart, Pfaffenwaldring 55, D-70569 Stuttgart, Germany
e-mail: bernd.hartke@rus.uni-stuttgart.de

Received: 24 February 1998 / Accepted: 6 March 1998 / Published online: 17 June 1998

Abstract. By an application to small silicon clusters Si_N (with N = 4,5,7,10) it is shown that truly *global* geometry optimization on an ab initio or density functional theory level can be achieved, at a computational cost of approximately 1–5 traditional local optimization runs (depending on cluster size). This extends global optimization from the limited area of empirical potentials into the realm of ab initio quantum chemistry.

Key words: Global geometry optimization – Silicon clusters – Model potentials

1 Introduction

There are two central problems in global cluster geometry optimization. One of these problems is the approximately exponential growth of the number of local minima with cluster size; this has been found empirically for small Lennard-Jones clusters [1, 2]. It has been argued that this might be an artifact of the Lennard-Jones potential. It is, however, likely that a scaling of a similar nature will prevail independent of the potential, since even simpler subproblems turn out to be of similar complexity. For example, the task of finding the three-dimensional arrangement of points given their pairwise distances has been shown to belong to the class of non-polynomial (NP) complete problems [3]. This strong scaling cannot be avoided even with modern global optimization techniques, e.g. refined genetic algorithm (GA) methods [4]. This problem of an explosive search space growth can only be overcome by an equally massive restriction of search space, using a suitable mixture of external information, higher level descriptions [5] and intelligent, adaptive growth strategies [6]. This is *not* the aim of this article.

The second problem is the strong dependence of the number of local minima and the geometries of the minimum cluster structures on details of the potential. This problem has been well known since the famous comparison of Lennard-Jones clusters with Morse clusters [7]. Even very elaborate empirical potentials [8] turn out to contain obviously wrong global minima [9]. Therefore, ab initio treatments are ultimately inevitable, but they are orders of magnitude more expensive than empirical potentials. Since every global optimization method requires *very many* evaluations of the potential, it seems completely illusionary to attempt global geometry optimizations on an ab initio level. Nevertheless, exactly this can be done, and it is the aim of this article to prove this via an actual application to a realistic problem.

In a previous publication [9], a strategy was presented that was designed to circumvent the second problem. Global geometry optimization on a model potential is done in parallel with (global) optimization of the parameters of this model potential. This is done by minimization of the differences between model and ab initio energies at the minimum structures found during the global geometry optimization. In this way, the expensive global optimization work is relegated to the cheap model potential domain, leaving only a few local optimizations in the ab initio domain. At the same time, the model potential is fit progressively better to ab initio data, as the algorithm proceeds. This method actually worked as expected for small silicon clusters. However, in order to save computational time, the ab initio potential was replaced by the complicated Bolding-Andersen empirical potential [8], while the much simpler Stillinger-Weber potential [10] in the modification of Gong [11] was used as the model potential. In fact, this strategy turned out to be even more powerful than expected. It found several "new" global minima on the Bolding-Andersen surface that had escaped the attention of its original authors; these minima were confirmed later in an independent study [12].

In this article, it is demonstrated that this strategy also works for an actual ab initio or, in this case, density functional theory (DFT) potential, again for the example of small silicon clusters. It is also demonstrated that the expense for this type of global optimization typically is in the order of a few local optimizations. Hence, global geometry optimization at the ab initio level becomes feasible even for systems of non-trivial size.

Obviously, this strategy depends on how well the model potential approaches the ab initio potential. As demonstrated previously [9], a perfect fit is not necessary; in fact, it is not even necessary that there is a one-to-one relation between minima on the model potential and minima on the ab initio potential, nor is a correct energy ordering of the minima on the model potential required. It is sufficient that within the basin of attraction of the global minimum on the ab initio potential there is also an important minimum on the model potential (i.e. a minimum that has some reasonable chance of being found in a global minimization – this is not necessarily the global minimum itself, since practical global minimizations are not perfect, but typically a low-lying local minimum). This places a lower limit on the appropriateness of the model potential function. But there are also upper limits on the goodness-of-fit and the complexity of the model potential. If the model potential matches the ab initio potential perfectly, no parameter optimization of the model potential is needed, and the task of global optimization on the ab initio potential reduces to a global optimization exclusively on the model potential. In this case, however, the computational expense of verifying such a perfect fit will be about as large as conducting a global optimization on the ab initio potential. Also, in practical applications of complex model potentials with very many parameters, it may become difficult to find reasonable intervals within which the parameters can be varied without destroying the suitability of the model potential. In spite of its importance, this topic of determining appropriate model potentials is beyond the scope of the present article; it will be dealt with in future investigations.

It should be emphasized that this paper is meant as a demonstration of the feasibility of the proposed method. In particular, it is shown that the method leads to a low, controlled computational expense while retaining a degree of global convergence sufficient for normal practical purposes. This paper is definitely not intended as a global survey of the potential energy surface of small silicon clusters, at whatever level of theory. Instead, it is deemed sufficient to show that the method yields most of the minima found in other, larger DFT or ab initio studies, albeit at a smaller computational expense and with greater confidence in global convergence. Also, the results presented are definitely not the ultimate ab initio answer to the silicon cluster structure question. Preliminary state-averaged complete active space self-consistent field (CASSCF) and multi-reference configuration interaction (MRCI) calculations in our group [13] have shown that, at least in the smallest clusters, several electronic configurations significantly contribute to the wavefunction in large regions of the cluster configuration space. Hence, single-reference treatments as they are done here and throughout most of the existing literature on this topic may not be very realistic.

2 Method

For a better understanding of the results shown later, here is a short description of the algorithm, as presented in Ref. [9]. The algorithm consists of two main stages or phases. In phase I, cluster geometries are globally optimized on the model potential, and at the same time, the model potential parameters are optimized globally with respect to ab initio (or DFT) single-point calculations, by iterating the following steps:

1. Initialization: calculate model energy $E_{\mathrm{mod},i}$ and ab initio energies $E_{\mathrm{true},i}$ for n random geometries.
2. Use a GA [6, 14–16] to optimize the model potential parameters globally, by minimizing $\sum_{i=1}^{n}(E_{\mathrm{mod},i} - E_{\mathrm{true},i})^2$ for all n geometries.
3. Choose a new random geometry.
4. Optimize this geometry globally on the model potential (with the parameters found in step 2) using molecular dynamics simulated annealing (MD-SA) [17–21] with incomplete cooling, followed by local refinement. This leads to a new geometry: $n \leftarrow n + 1$.
5. Calculate $E_{\mathrm{mod},n}$ and $E_{\mathrm{true},n}$ for the resulting geometry.
6. Go to step 2, until the model potential parameters are converged and until n is large enough.

In the applications below, we use a fixed value of $n_{\max} = 100$; the results shown give an impression of which values of $n_{\max}$ would have been sufficient in each case. There is no need to have a GA [6, 14–16] and SA [17–21] in steps 2 and 4, respectively. They were used here only because subroutines of this type were available that had been applied previously in similar cases with success. In principle, they can be replaced by any other global optimization method that works comparably well. The MD-SA in step 4 is incomplete on purpose; on the one hand, this avoids the slow, inefficient final optimization phase that is more efficiently done by a local optimization routine. On the other hand, it avoids repetitious re-discoveries of the same minimum and allows for exploration of other low-lying local minima of the model potential.

Phase II of the algorithm proceeds as follows:

1. Order the n resulting geometries of phase I by ab initio energy.
2. Perform local ab initio (or DFT) optimizations of those structures with the lowest energies that appear likely to lead to different final structures.

The resulting final structures will correspond to energetically low-lying local minima on the ab initio (or DFT) surface and will also include the global minimum with high probability.

Typically, global convergence of global optimization algorithms can be proven only for an infinite effort (e.g. for infinitely long trajectories with an exponential cooling schedule in SA [18]). Therefore, in all practical global optimizations, there is never a guarantee of finding the true global optimum (except in problems of trivial size where it is possible to enumerate all minima). Hence, the fact that this algorithm can locate the global minimum "only" with some probability is not a disadvantage but a typical feature that is to be expected. As shown in this article and in the previous test application [9], the probability of locating the global minimum is high for the examples given.

The presented algorithm is admittedly of a simple nature. Also, a non-iterated version of it may be similar to what many researches typically do to locate global or low-lying local minima: (local or global) pre-optimization on an empirical potential or with semi-empirical methods, followed by a series of local ab initio optimizations. One novelty of the present approach lies in the adaption of the model potential to the ab initio data (in this respect the method resembles recent attempts to re-parametrize semiempirical methods in order to achieve improved performance of these methods for a specific, given system [22, 23]) and in the SCF-like iteration, alternating between re-parametrization and geometry optimization, ensuring that the fit of the model potential to the ab initio data is done not at arbitrary points but in the interesting regions close to the minimum structures. Furthermore, in the first tests [9], this simple algorithm turned out to be more powerful than expected. Therefore, it is interesting to study its performance in a realistic example.

3 Application

In order to be able to judge the success of the algorithm, we focus again on small silicon clusters, where there is at least some degree of consensus in the literature on what the global minimum structures are. Also, there are by now a few experimental results, supporting some of the theoretically predicted structures.

Single-point calculations and local geometry optimizations of the clusters were done at the DFT level of theory, in the restricted Kohn-Sham formalism [24] with B3LYP-treatment [25] of the exchange-correlation part. To speed up the calculations, in phase I, the neon core of each silicon atom was replaced by the ECP10MWB pseudopotential of Stoll and coworkers [26], with the remaining valence electrons being represented by the corresponding *s*- and *p*-orbital basis set, to which a *d*-orbital from Woon and Dunning's correlation-consistent polarized valence double-zeta (*cc*-pVDZ) basis [27, 28] was added. In phase II, for Si_4 and Si_7, all electron calculations were performed, using the full *cc-p*VDZ basis. At this stage, also other basis sets (6-31G* and *cc-p*VTZ) were tested, but this did not change the results qualitatively and had only marginal quantitative effects (about 0.6 or 0.02 Å change in bond lengths and about 0.3 or 3° change in bond angles, in the locally optimized structures).

This DFT treatment is realized by linking the global optimization algorithm described above with standard quantum chemistry packages: MOLPRO [29] for the single-point calculations in phase I, and Gaussian 94 [30] for the local DFT optimizations in phase II.

As in the previous test application [9], the model potential is again the Stillinger-Weber-Gong potential [10, 11], since it proved itself to be surprisingly versatile there. As hinted at in the introduction, the Bolding-Andersen potential is less practical as a model potential for the present purpose, since it contains 40 parameters with a large degree of interdependence between them, which makes it difficult to vary the potential while keeping its overall form reasonable.

4 Results

Results for Si_7, Si_4, Si_6 and Si_{10} are presented in this section, in the order of increasing challenge for the global optimization.

Table 1 displays a detailed overview of the results for Si_7, supplemented by Fig. 1. The geometry Si7.1 proposed by the algorithm as the global minimum is a pentagonal bipyramid; this agrees with almost all published calculations on various levels of theory, e.g. empirical potentials [31, 32], extended-Hückel [33], DFT-MDSA [35, 34], fourth-order Møller-Plesset perturbation theory (MP4) and Hartree-Fock (HF)-SCF [36], and it is also in accord with the recent experimental findings [37, 38]. This apparent independence of the computational method used seems to indicate that the Si_7 problem is simple. However, in our previous test application [9], the present global optimization method with the very same Stillinger-Weber-Gong model po-

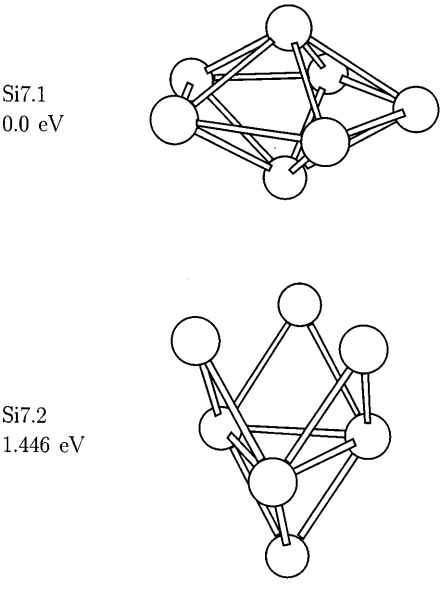

Fig. 1. Optimized geometries of Si_7: Si7.1 is the (very likely) global minimum, Si7.2 is a low-energy local minimum (cf. Table 1). Energies in eV are given relative to Si7.1

Table 1. Result of the global DFT geometry optimization of Si_7

n[a]	E-No.[b]	Geometry[c]	Opt. geometry[d]	E_{opt}/eV[e]	Steps[f]
1	19	Pent. bipy.	Si7.1	0.0	6
12	14	Pent. bipy.	Si7.1	0.0	6
14	20	Pent. bipy.	Si7.1	0.0	6
77	22	Capped Td	Deformed Si7.2	0.6539	16
68	1	Pent. bipy.	Si7.1: pent. bipy.	0.0	4
80	25	Irregular[g]	Deformed Si7.2	0.8382	25
91	26	Capped Oh	Si7.2: C_{3v}	1.446	9

[a] Generated in the *n*'th step of phase I
[b] Ranking by increasing DFT energies after phase I
[c] Geometry generated in phase I: pent.bipy, pentagonal bipyramid; Td, tetrahedron; Oh, octahedron
[d] Result of the local optimization in phase II; geometries denoted as Si7.n are shown in Fig. 1
[e] DFT energy after phase II, relative to the pentagonal bipyramid Si7.1
[f] Number of steps in the local optimization of phase II
[g] Pentagonal bipyramid with one equatorial atom moved to an equatorial capping position

tential was able to locate a planar artifact that has a lower energy than the pentagonal bipyramid on the Bolding-Andersen surface. Similar planar structures did not appear during the global optimization on the DFT surface. This proves that the model potential parameter optimization in the present method actually adapts the model potential successfully to the more complicated potential it is meant to simulate (i.e. to the Bolding-Andersen potential in the previous test application [9], or to the DFT potential in the present study). This appearance of artifacts also shows that even in the apparently simple case of Si_7 a more traditional approach of running a series of local optimizations starting from geometries based on reasonable guesses or on pre-optimizations using fixed-parameter model potentials may be misleading. At least, it prevented Bolding and Andersen from locating these artifacts on their surface [8].

Table 1 also shows that the global optimization on the model potential in phase I yields very good starting geometries for the ensuing local DFT optimizations in phase II. The regular structures Si7.1 and Si7.2 can be fully converged within 4–9 steps, whereas 15–20 steps are needed for re-convergence if one of these geometries is distorted by randomly applying coordinate changes in the order of 0.1 Å.

The computational expense should be compared with that of the standard approach of a series of local DFT optimizations starting from geometries generated by educated guesswork (possibly supported by pre-optimizations with lower-level methods or on fixed model potentials). Each geometry in phase I needs one single-point DFT energy calculation, hence when arriving at geometry number n in this phase, n DFT energy calculations have been made. The local optimization on the DFT level in phase II needs gradients, therefore we assume that each local optimization step in this phase requires a computational expense equivalent to approximately two energy calculations. The geometry number 68 reached the best DFT energy after phase I, and could be converged locally in phase II in only 4 steps. This corresponds to a total expense of 80 energy calculations (4 DFT energy calculations for the random geometries in the startup of phase I, plus 68 in the execution of phase 1, plus 2×4 in the local optimization of phase II). Assuming that a typical starting geometry in the traditional approach can be converged in only 10 steps (corresponding to 20 energy calculations), this allows us to test only 4 starting geometries in this approach; that is, the global optimization with the present method appears to be as expensive as 4 local optimizations. However, inspecting Table 1 again, it is not really necessary to wait for geometry number 68 in phase I, since geometries 1, 12 and 14 also converge to the same final structure in phase II. Therefore, our estimate is overly conservative; we can also find geometry Si7.1 with a computational expense of only 10–20 energy calculations. With this estimate, the global geometry optimization is only as expensive as a single local optimization.

Si_4 is a smaller cluster than Si_7, but it is actually more difficult for global optimization since different methods have led to different results. Several simple empirical potentials favour the tetrahedron, more elaborate ab initio approaches arrive at the rhombus instead [8, 39]. Table 2 and Fig. 2 show that the present algorithm needs about 30–50 energy calculations to find the planar rhombus Si4.1 as global minimum, in agreement with other DFT and ab initio results [35, 40, 41] and experimental values [37, 38]. Therefore, with the same assumptions as above, the global DFT optimization succeeds with an expense of only 1.5–2.5 local minimizations.

The difficulty posed by Si_6 is not the existence of several distinct minimum structures that are hard to find but a competition of several closely related structures in a very flat region of the potential: a pentagonal bipyramid with one equatorial atom missing (pb-1, often referred to as bicapped tetrahedron), the square bipyramid (compressed octahedron), and the equatorially edge-capped trigonal bipyramid. All of these structures are close to the octahedron, but the octahedron itself is usually found at a clearly higher energy, except on some empirical potentials [8, 31]. Which of these structures becomes the global minimum depends very strongly on the method used [34, 36, 38, 41–43].

Clearly, this dispute can only be settled by a high-level (and possibly multi-reference) treatment of electron correlation. Nevertheless, it is satisfying that the present method applied on the moderate DFT level is able to reveal the complete picture of the Si_6 surface exactly as just sketched, cf. Table 3 and Fig. 3. The pb-1 structure Si6.1 and the square bipyramid Si6.2 are very close competitors for the global minimum; the energetic dif-

Table 2. Result of the global DFT geometry optimization of Si_4

n[a]	E-No.[b]	Geometry[c]	Opt. geometry[d]	E_{opt}/eV[e]	Steps[f]
14	17	Planar Rh	Si4.1	0.0	5
35	1	Planar Rh	Si4.1: planar Rh	0.0	4
52	24	Triangle + 1	Si4.1	0.0	13
56	46	Tetrahedron	Si4.2	2.354	3
66	3	Bent Rh	Si4.1	0.0	9

[a] Generated in the n'th step of phase I
[b] Ranking by increasing DFT energies after phase I
[c] Geometry generated in phase I: Rh, rhombus; triangle + 1, triangle with one appended atom = opened rhombus
[d] Result of the local optimization in phase II; geometries denoted as Si4.n are shown in Fig. 2
[e] DFT energy after phase II, relative to the planar rhombus Si4.1
[f] Number of steps in the local optimization of phase II

ference between them is certainly not significant compared to the inaccuracies of the DFT approach used. A capped trigonal bipyramid is also found, albeit in distorted form and with a non-equatorial cap (Si6.3; it is likely that a structure with an equatorial cap may have a similar energy. This question was not investigated further, since a full surface characterization is not the aim of this study). The octahedron Si6.4 is correctly identified as a high-lying local minimum; its minor importance is further documented by geometry number 11 managing to escape from its neighbourhood in configuration space and by other, less symmetric geometries like Si6.3 occuring at much lower energy. Using the same assumptions as above, the computational expense for finding the structure Si6.1 is comparable to that of two local optimization runs.

Si_{10} is a substantially larger cluster, and there has been some disagreement about its global minimum structure [8, 33, 34, 36, 42, 43]. Recently, there seems to be some convergence of theoretical [44] and even experimental work [45] towards the tetracapped trigonal prism (ttp) as the global minimum. Application of the present strategy to Si_{10} yields the results shown in Table 4 and Fig. 4. Obviously, there is again qualitative agreement with the currently accepted results. The ttp structure Si10.1 (or possibly a skewed variant of it, Si10.2) is found as the global minimum, followed by the bicapped square antiprism Si10.3, also sometimes proposed in the literature as the global minimum. The computational effort to find the ttp structure amounts to 98 energy calculations. If we assume in all fairness that a typical local optimization run now requires about 15–20 steps due to the cluster being larger, this estimate is equivalent to approximately 2.5–3 local optimization runs. Of course, it has to be expected that the effort

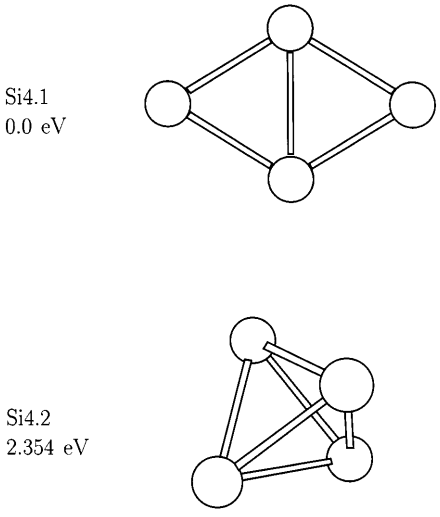

Fig. 2. Optimized geometries of Si_4: Si4.1 is the global minimum, Si4.2 is a low-energy local minimum (cf. Table 2). Energies in eV are given relative to Si4.1

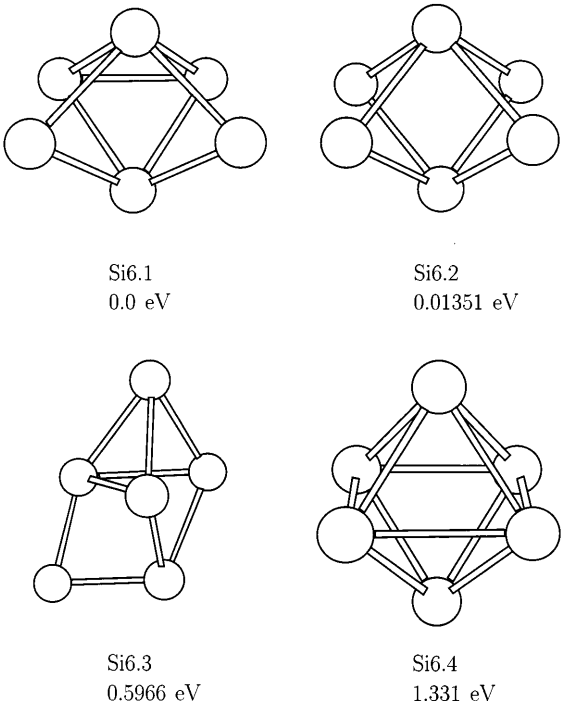

Fig. 3. Optimized geometries of Si_6: Si6.1 and Si6.2 are close competitors for the global minimum, Si6.3 is a low-energy local minimum, the octahedron Si6.4 is much higher in energy (cf. Table 3). Energies in eV are given relative to Si6.1

Table 3. Result of the global DFT geometry optimization of Si_6

n[a]	E-No.[b]	Geometry[c]	Opt. geometry[d]	E_{opt}/eV[e]	Steps[f]
6	2	pb-1	Si6.1: pb-1	0.0	15
8	43	tbp-1cap	Si6.3: dist.tbp-1cap	0.5966	11
11	50	Oh	Si6.2: sbp-c	0.01351	19
36	30	sbp-c	Si6.2: sbp-c	0.01351	15
62	45	sbp-e	Si6.2: sbp-c	0.01351	18
67	1	pb-1	Si6.1: pb-1	0.0	15
90	51	Oh	Si6.4: Oh	1.331	4

[a] Generated in the n'th step of phase I
[b] Ranking by increasing DFT energies after phase I
[c] Geometry generated in phase I: pb-1, pentagonal bipyramid with one equatorial atom missing; sbp-c/e, square bipyramid (compressed or elongated octahedron); tbp-1cap, trigonal bipyramid with one non-equatorial edge capped; dist., distorted; Oh, octahedron
[d] Result of the local optimization in phase II; geometries denoted as Si6.n are shown in Fig. 3
[e] DFT energy after phase II, relative to the sbp-1 structure Si6.1
[f] Number of steps in the local optimization of phase II

Table 4. Result of the global DFT geometry optimization of Si_{10}

n[a]	E-No.[b]	Geometry[c]	Opt. geometry[d]	E_{opt}/eV[e]	Steps[f]
24	2	pp + rhombus	Si10.2: skew-ttp	0.09562	19
25	7	absa	Si10.3: absa	0.8438	12
40	3	pp + rhombus	Si10.1: ttp	0.0	27
54	1	dist.ttp	Si10.4: csp + rhombus	1.120	18

[a] Generated in the n'th step of phase I
[b] Ranking by increasing DFT energies after phase I
[c] Geometry generated in phase I: pp, pentagonal pyramid; ttp, tetracapped trigonal prism; absa, axially bicapped square antiprism; dist., distorted; csp, equatorially edge-capped square pyramid
[d] Result of the local optimization in phase II; geometries denoted as Si10.n are shown in Fig. 4
[e] DFT energy after phase II, relative to the ttp structure Si10.1
[f] Number of steps in the local optimization of phase II

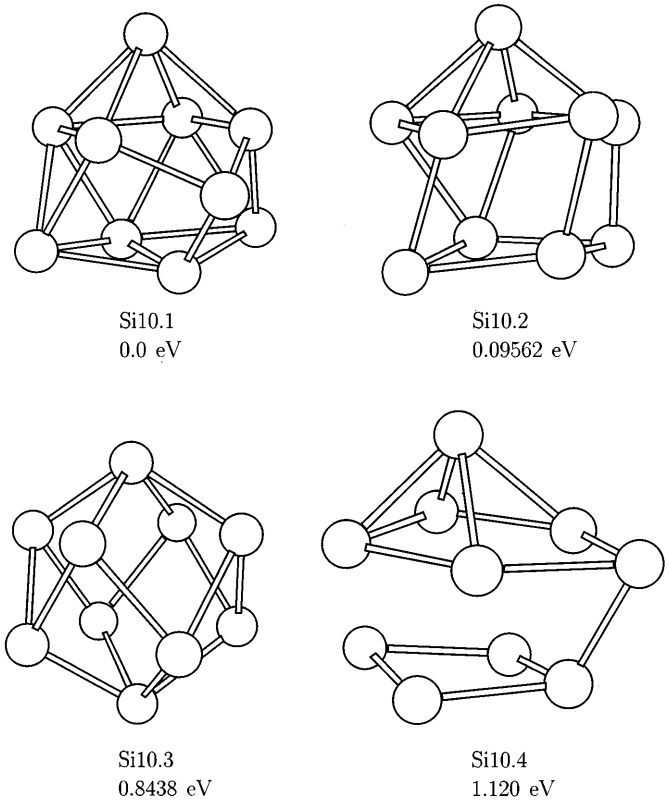

Fig. 4. Optimized geometries of Si_{10}: Si10.1 is presumably the global minimum, but the distorted variant Si10.2 is very close in energy, Si10.3 and Si10.4 are low-energy local minima (cf. Table 4). Energies in eV are given relative to Si10.1

increases with cluster size, because the number of local minima increases presumably exponentially. As explained in the introduction, an additional methodical development is necessary to overcome this difficulty.

5 Discussion

We have shown that the strategy presented here allows for actual global geometry optimization on an ab initio (or DFT) level, as evidenced by our finding most of the currently accepted important minimum structures for the clusters studied here. Nevertheless, the computational effort is not larger than that of a few local optimizations (on that level of theory).

As already pointed out in the introduction, this is not a claim that the minimum structures shown here actually correspond to the "true" global minima on a sufficiently high level of theory, although these structures agree with the most recent ones proposed in the literature. On the contrary, high-level ab initio calculations for small silicon clusters performed in our group [13] indicate that multi-reference treatments are necessary, and currently we do not know if any of the structures shown will survive as global or low-lying local minima under such a treatment. With the techniques of this article, however, we hope to be able to perform global optimizations even at this level of theory.

Currently, we are extending this technique to molecular clusters, with applications to small water clusters.

On the methodical side, the surprising success of the simple Stillinger-Weber-Gong potential in this article and in the earlier study [9] calls for an investigation of exactly how flexible a model potential functional form has to be in order to perform well in a strategy such as the one presented here. This will be addressed by future work.

Also, this method does not address the first of the two central problems of global cluster geometry optimization mentioned at the beginning of this article, namely the explosive growth of computational expense with cluster size. First steps to alleviate this problem have already been made in our group [6], and further work along these lines is in progress.

Acknowledgements . Financial support in connection with this work by the DFG "Schwerpunktprogramm Molekulare Cluster" is gratefully acknowledged.

References

1. Hoare MR (1979) Adv Chem Phys 40: 49
2. (a) Stillinger FH, Stillinger DK (1990) J Chem Phys 93: 6106; (b) Wille LT, Vennik J (1985) J Phys A 18: L419; L1113
3. Hendrickson BA (1995) SIAM J Opt 5: 835
4. Gregurick SK, Alexander MH, Hartke B (1996) J Chem Phys 104: 2684
5. Mestres J, Scuseria GE (1995) J Comp Chem 16: 729
6. Hartke B (1995) Chem Phys Lett 240: 560
7. Hoare MR, McInnes JA (1983) Adv Phys 32: 791

8. Bolding BC, Andersen HC (1990) Phys Rev B 41: 10568
9. Hartke B (1996) Chem Phys Lett 258: 144
10. Stillinger FH, Weber TA (1985) Phys Rev B 31: 5262
11. Gong XG (1993) Phys Rev B 47: 2329
12. Niesse JA, Mayne HR (1996) Chem Phys Lett 261: 576
13. Baumhauer M (1996) diploma thesis, University of Stuttgart, Stuttgart, Germany
14. Holland JH (1975) Adaption in natural and artificial systems. University of Michigan Press, Ann Arbor, Mich
15. Goldberg DE (1989) Genetic algorithms in search, optimization and machine learning. Addison-Wesley, Reading, Mass
16. Hartke B (1993) J Phys Chem 97: 9973
17. Kirkpatrick S, Gelatt CD Jr, Vecchi MP (1983) Science 220: 671
18. van Laarhoven, PJM, Aarts EHL (1987) Simulated annealing: theory and applications. Reidel. Dordrecht
19. Hartke B, Carter EA (1992) J Chem Phys 97: 6569
20. Ingber L (1989) Math Comput Modelling 12: 967
21. Basu A, Frazer LN (1990) Science 249: 1409
22. Rossi I, Truhlar DG (1995) Chem Phys Lett 233: 231
23. Peslherbe GH, Hase WL (1996) J Chem Phys 104: 7882
24. Parr RG, Yang W (1989) Density functional theory of atoms and molecules. Oxford University Press, New York
25. (a) Becke AD (1993) J Chem Phys 98: 1372, 5648; (b) Stephens PJ, Devlin FJ, Chabalowski CF, Frisch MJ (1994) J Phys Chem 98: 11623
26. Bergner A, Dolg M, Küchle W, Stoll H, Preuss H (1993) Mol Phys 80: 1431
27. (a) Dunning TH Jr, (1989) J Chem Phys 90: 1007; (b) Peterson KA, Kendall RA, Dunning TH Jr (1993) J Chem Phys 99: 9790
28. Woon DE, Dunning TH Jr (1993) J Chem Phys 98: 1358
29. MOLPRO is a packet of ab initio programs, written by Werner HJ, Knowles PJ, with contributions by Amos RD, Berning A, Cooper DL, Deegan MJO, Dobbyn AJ, Eckert F, Hampel C, Leininger T, Lindh R, Lloyd AW, Meyer W, Mura ME, Nicklass A, Palmieri P, Peterson K, Pitzer R, Pulay P, Rauhut G, Schütz M, Stoll H, Stone AJ, Thorsteinsson T
30. Gaussian 94, Revision E.2. Frisch MJ, Trucks GW, Schlegel HB, Gill PMW, Johnson BG, Robb MA, Cheeseman JR, Keith T, Petersson GA, Montgomery JA, Raghavachari K, Al-Laham MA, Zakrzewski VG, Ortiz JV, Foresman JB, Cioslowski J, Stefanov BB, Nanayakkara A, Challacombe M, Peng CY, Ayala PY, Chen W, Wong MW, Andres JL, Replogle ES, Gomperts R, Martin RL, Fox DJ, Binkley JS, Defrees DJ, Baker J, Stewart JP, Head-Gordon M, Gonzalez C, Pople JA (1995) Gaussian, Inc., Pittsburgh Pa
31. (a) Chelikowsky JR, Phillips JC (1990) Phys Rev B 41: 5735; (b) Chelikowsky JR, Glassford KM, Phillips JC (1991) Phys Rev B 44: 1538
32. Mistriotis AD, Flytzanis N, Farantos SC (1989) Phys Rev B 39: 1212
33. Slee T, Zhenyang L, Mingos DMP (1989) Inorg Chem 28: 2256
34. (a) Ballone P, Andreoni W, Car R, Parrinello M (1988) Phys Rev Lett 60: 271; (b) Röthlisberger U, Andreoni W (1991) Z Phys D 20: 243
35. Binggeli N, Chelikowsky JR (1994) Phys Rev B 50: 11764
36. Raghavachari K, Rohlfing CM (1988) J Chem Phys 89: 2219
37. Li S, van Zee RJ, Weltner W Jr, Raghavachari K (1995) Chem Phys Lett 243: 275
38. Honea EC, Ogura A, Murray CA, Raghavachari K, Sprenger WO, Jarrold MF, Brown WL (1993) Nature 366: 42
39. Andreoni W, Pastore G (1990) Phys Rev B 41: 10243
40. Fournier R, Sinnott SB, DePristo AE (1992) J Chem Phys 97: 4149
41. (a) Raghavachari K, (1985) J Chem Phys 83: 3520; (b) Raghavachari K (1986) J Chem Phys 84: 5672
42. (a) Li S, Johnston RL, Murrell JN (1992) J Chem Soc Faraday Trans 88: 1229; (b) Wales DJ, Waterworth MC (1992) J Chem Soc Faraday Trans 88: 3409
43. Patterson CH, Messmer RP (1990) Phys Rev B 42: 7530
44. Raghavachari K, Rohlfing CM (1992) Chem Phys Lett 198: 521
45. Rantala TT, Jelski DA, George TF (1995) Chem Phys Lett 232: 215